7th Int. Symp. "Nanostructures: Physics and Technology"
St Petersburg, Russia, June 14–18, 1999

Radiative processes in InGaN quantum wells

P. G. Eliseev
Center for High Technology Materials, University of New Mexico, Albuquerque, NM 87106 U.S.A. (on leave from P. N. Lebedev Physics Institute, Moscow)

Abstract. Light-emission properties of InGaN quantum wells are reviewed and discussed including performance in wide range of temperatures (up to 450 K). The typical anomaly of "blue" temperature-induced shift of the luminescence spectral peak is explained in terms of the band-tail model. The model is applied to the InGaN active medium in LEDs and in lasers. The tail states are associated with composition variations in the alloy. They seem to be favorable for efficient radiative recombination.

1 Introduction

Most of new impressive achievements in the short-wavelength semiconductor optoelectronics (high-efficiency violet, blue and green LEDs [1], UV and purple LDs [2–5]) are associated with utilization of InGaN quantum wells (QWs). Early studies of InGaN alloy had been performed with polycrystalline films deposited on sapphire or fused quartz (see, for example [6, 7]). The wavelength coverage had been established from $\sim$ 365 nm (GaN) to $\sim$ 620 nm (InN). During last decade, the quality of InGaN material is improved significantly. Quantum efficiency of the luminescence in this material is high and comparable to that in high-quality GaAs and InGaAs.

The InGaN alloy is known as an unstable system at substantial content of indium, therefore, it can be subjected to decomposition or phase modification. Occurrence of phase separation is established under the annealing procedures [7]. Theoretically, the immiscibility in InGaN had been predicted [8]. There is no available commercial substrate material for lattice-matched growth, and most of devices are fabricated using mismatched substrates like sapphire or SiC. As a result, the lattice perfection is low, with dislocation density as high as 10^9–$10^{12}\,\mathrm{cm}^{-2}$. In spite of this, InGaN QWs demonstrate excellent radiative characteristics. Nitride-based semiconductor device are expected to operate well above the room temperature. There is a challenge for future optoelectronics to face applications at elevated temperatures. InGaN-based devices are most promising candidates for this purpose [9]. In addition, semiconductor nitrides are known as piezoelectric materials [10]. Therefore, some novel properties can be expected in InGaN associated with stress-induced piezoelectric fields. Thus the understanding of radiative processes in InGaN is of great interest.

2 Quantum efficiency and high-temperature performance of LEDs

An important subject of discussion is quantum efficiency of the InGaN-based LEDs. The external quantum efficiency of visible LEDs at room temperature is 5–7% in commercial samples and up to 12% in experimental samples. Commercial LEDs shows very slow degradation or no visible degradation. Therefore, they are capable to operate long time at rather high optical output.

L–I characteristics are shown of green commercial LEDs in Fig. 1 in the temperature range [9]. The optical power measurements are made under dc injection below the current of 10 mA (current density $J \sim 14\,\mathrm{A/cm}^2$) and in pulse-current (pc) injection at higher

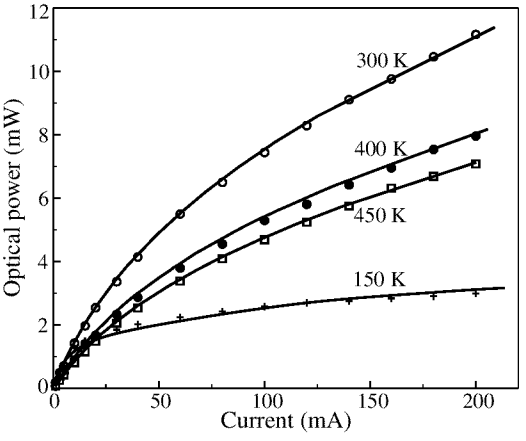

Fig. 1. Light-current characteristics of green Nichia InGaN SQW LED in temperature range up to 450 K. Curves are calculated with recombination coefficients as fitting parameters. Diode area is 7×10^{-4} cm^2.

current to avoid overheating. In addition to the power measurements the carrier lifetime is measured at 300 K. This gives sufficient experimental information to consider the recombination balance in SQW LEDs and to obtain the fitting of the room-temperature L–I curve assuming standard terms of linear non-radiative recombination, "bimolecular" radiative recombination, the Auger recombination and some higher-order recombination term which will be discussed later. For other temperatures than 300 K we perform similar analysis assuming that the radiative recombination coefficient B is in reverse proportion to the temperature as it is expected for 2D system. This theory need experimental confirmation because operating states in InGaN QWs are not obviously 2D states, but can be quantum-dot-like states. It may be reasonable for most low-energy states occupied at low current. In Ref. [11] the radiative lifetime is found to be not temperature dependent between 10 K and about room temperature in InGaN with indium content of $\sim$ 2%. This is considered as an indication on 0D nature of involved states. Therefore, the hypothesis of constant B should be also considered. The equation used in the analysis is as follows:

$$J/e = AN + BN^2 + CN^3 + DN^{4.8} + EN^9 + \ldots \tag{1}$$

where N is 2D carrier density, A, B, C, D and E are fitting coefficients. The quantity A relates to the linear non-radiative recombination, C is the Auger coefficient, high-order coefficients D and E describe non-radiative losses due to leakage of carriers from active region and overflow losses, respectively.

The fitting parameters are shown for green LED at three temperatures in Table 1. The coefficient D is probably accounted for the leakage processes from the quantum well. Understanding that the potential barriers are very high in this structure, the leakage can be associated with not over-barrier leakage but with a transport via defects. The quantity D appears to decrease with temperature rise, whereas the contribution into the recombination balance increases. The decrease of D can be associated with a decrease of the carrier degeneracy which influence the effective height of the potential barrier for carriers. Process described by coefficient E is seen at low temperatures and disappears at room temperature. Because the small thickness of the quantum-well layer (3 nm), it can be associated with overflow when the free path of carriers is larger than QW thickness.

Table 1. Fitting parameters used to fit the L–I curves of green LED. All coefficients are used in the 2D recombination balance therefore they relate to the 2D carrier density in the QW.

Temperature, K	A, 1/s	B, cm^2/s	C, cm^4/s	D, cm$^{7.6}$/s	E, cm^{16}/s
100	$< 1\times10^{6}$	3×10^{-4}	$< 5\times10^{-18}$	$< 2\times10^{-37}$	7×10^{-86}
300	3×10^{6}	1×10^{-4}	$< 2\times10^{-17}$	5×10^{-39}	$< 1\times10^{-90}$
450	2.8×10^{7}	6.67×10^{-5}	$< 5\times10^{-17}$	4.5×10^{-39}	$< 1\times10^{-90}$

The LED performance at 450 K indicates possible high-temperature applications. In frames of above mentioned analysis we see that the internal quantum efficiency at room temperature can be estimated as 66.9% at 20 mA and 27.7% at 200 mA. At 450 K these figures are 40.3% and 18.6% respectively. The efficiency extraction and collection of photons is estimated as $\sim$ 8%. This corresponds to the external quantum efficiency of 5.35% (300 K) and 3.22% (450 K) at 20 mA. The calculated carrier lifetime in green InGaN SQW LED at 20 mA at room temperature is $\sim$ 6 ns (radiative lifetime is 9.2 ns), measured value is 6.2$\pm$0.5 ns. This shows satisfactory agreement of the proposed recombination balance with experimental data.

3 EL and PL spectra

From systematic study we point out following features of the spectra: 1) spectral peak position is typically not in agreement with nominal levels of quantum-confined states in quantum wells but is substantially red-shifted; 2) large bandwidth (typically, from $5.5kT$ to $9kT$ at 300 K in green LEDs depending on the injection current); 3) strong "blue" shift along with increase of the current (about 200 meV in green LEDs when current goes from 0.5 A/cm^2 to $\sim$ 2 kA/cm^2); 4) non-monotone (S-shaped) temperature dependence of the peak position with gradual "blue" temperature-induced shift which occurs in contrast to the expected temperature-induced band-gap shrinkage. The anomaly in the temperature behavior of the spectral peak position was reported in Ref. [12] in the study of the spontaneous electroluminescence spectra of InGaN-based SQW LEDs under strong current pulses. At low current this anomaly is even more apparent. In Fig. 2 the spectral peak position is shown in the blue LED under different values of the current. The interpretation of this behavior has been given in [13] in terms of the band-tail model.

The photoluminescence data are shown here in context of the anomaly of "blue" temperature-induced shift that was mentioned above in connection with electroluminescence. It is found in several papers that the shift is rather common in different structures: single heterostructures, double heterostructures (with over-critical bulk-like thickness up to 40–50 nm) and in quantum wells (thickness is 2–5 nm). The spectral peak position in function of temperature is shown in Fig. 3 for two different epitaxial structures. The anomaly is identified which is temperature "blue" shift in the range of 50–150 K in sapphire-substrate sample. This is not typical for undoped GaN, but is well pronounced in most InGaN luminescent structures including those in green LEDs investigated by both EL and PL characterization techniques [13]. Homoepitaxial sample does not show temperature-induced "blue shift" anomaly in the same temperature range.

4 Band-tail model

The InGaN-based materials, including both QW and more thick layers, are subjected to the significant broadening due to non-uniformity of the alloy composition (in addition to the defect-related and impurity-related broadening expected in both GaN and InGaN). In ideal QW, the DOS at the band edge is described by step-like function. When the energy position

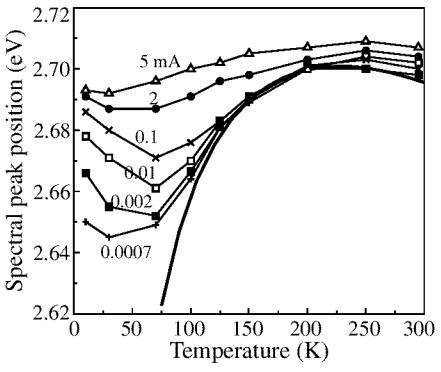

Fig. 2. EL spectral peak position of blue InGaN SQW LED at different current [13]. Thick curve is calculated according to Eq. (2). Fitting parameter s is 31.5 meV.

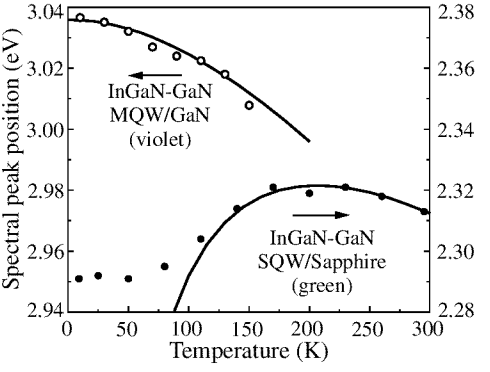

Fig. 3. PL spectral peak position of two InGaN samples: 1) open circles are for homoepitaxial MQW structure (grown by MOCVD on bulk GaN substrate obtained by sublimation method); pumping wavelength is 325 nm [18]; 2) solid circles are for green LED SQW structure on sapphire substrate; pumping wavelength is 442 nm [13].

of the band edge varies the averaged DOS becomes to be broadened and it is non-zero below the nominal band edge. We call this range the band tail. It is occupied by the excess carriers in first, and filling of the band-tail states gives blue shift of the spectral peak. The band tail in undoped InGaN is result of "anti-phase" variations of the band edges. This means that c-band edge is going down, whereas v-band edge is going up. This is opposite case as compared with heavily doped materials, where the edges vary "in-phase". In InGaN, carriers are captured into band-tail states (captured electron-hole pairs can be considered as localized exciton) and then recombine via vertical transitions. That carrier which is captured below the mobility edge in the tail is localized. It has greater chance to recombine radiatively as compared with mobile carriers. It can not diffuse freely and can not come to nonradiative center.

Applying the Gaussian statistics for the band-gap variations, one obtains an Erf-type distribution for averaged DOS. Therefore, the asymptotic part of DOS distribution can be described in term of the Gaussian tail (with the same dispersion as that of the assumed statistics). The tail states can be occupied in non-degenerated manner like states in an ordinary band. This means that most of carriers occupy states substantially above the quasi-Fermi level F. As DOS in non-zero below this level, some of carriers are degenerated there. Therefore in general, the carriers in the tail are degenerated partially, and the non-degenerated case means only the carriers predominate in non-degenerated state. The energy distribution function $N(E, F, T)$ of carriers in the tail is blue-shifted when temperature rises, and its peak position is much higher than F. When the DOS of electron and hole tails are the Gaussian functions the spectral peak is red-shifted in respect to the energy difference E_0 between the Gaussian centers. The shift is equal to σ^2/kT, where $\sigma^2 = \sigma_e^2 + \sigma_h^2$, and σ_e^2 and σ_h^2 are dispersions of DOS functions of electrons and holes, respectively [13]. In this case the peak position corresponds to equation

$$E_{\text{peak}}(T) = E_0(0) - \alpha T^2/(T + \beta) - \sigma^2/kT, \tag{2}$$

where first and second terms in the right side are the Varshni approximation for band-gap

with fitting parameters $E_0(0)$, α and β, and third term is temperature-dependent shift with band-tail parameter σ as explained above. This expression is a good approximation for low current above 100 K (non-degenerate occupation), whereas at low temperature and at high current it is not adequate because of the occupation degeneracy. We have inspected numerous reported data concerning the spectral peak position of InGaN emission (from QWs and bulky epilayer samples) versus temperature (both PL and EL measurements) and collected results of approximate analysis by the expression (2) in Table 2. Parameter $E_0(0)$ varies according to the average indium content. The band-tail parameter σ increases along with decrease of $E_0(0)$ suggesting the correlation of the composition variation with average indium content.

The Eq. (2) shows that the temperature dependence of the alloy bandgap can not be obtained from the luminescence peak position with no knowledge of σ. This explains difficulties of description of the InGaN bandgap parameters in spite of numerous PL and EL measurements published. Interesting experimental fact is that in homoepitaxial MQW samples of InGaN (grown on bulk GaN prepared by sublimation method) the "blue"-shift anomaly is not observed. Corresponding data are given in the last line in Table 2. It can be associated with lower dislocation density in bulky substrate. Simultaneously, these homoepitaxial structure does not demonstrate efficient luminescence, especially at room temperature. It seems to be an indication that tail states are favorable for radiative recombination, whereas in absence of tails, the radiative recombination is less competitive with non-radiative processes.

The band-tail approach is valid not only to InGaN quantum wells, but also to thick ("bulky") layers of InGaN grown on sapphire substrates. The approach seems to be adequate for both strained and relaxed structures. However, in non-relaxed structures the contribution of piezoelectric field is expected. The piezoeffect can produce shift of energy levels of 2D quantum-confined states that should be compared with the broadening parameter in order to understand if it is observable. There is also significant temperature-dependent homogeneous broadening of the emission band providing a masking of more fine effects. Large total spectral bandwidth of the InGaN emission is governed by both homogeneous and inhomogeneous contributions that combined in geometrical manner. Band-tail contribution into FWHM is $\sim 2.35\sigma$. As an example, in green LED, bandwidth of $\sim$ 160 meV is contributed by $\sim$ 80 meV from the band-tail broadening and $\sim$ 140 meV from the homogeneous (collisional) broadening.

5 About the role of dislocations

Dislocations can play an important role in the formation of In-rich clusters. They supply the centers of the phase precipitation and also produce a non-uniform inclusion of indium during growth. The low-temperature MOCVD epitaxial growth (typical to InGaN growth as compared with GaN growth) is shown to be associated with screw-type dislocation (spiral growth) [20, 21]. The growth rate and indium content are enhanced in vicinity of such dislocations. Therefore, dislocation density is one of important factors providing both compositional and geometrical variation in InGaN QWs. Large-size (0.1–1 μm) variations of the compositions near dislocations have been revealed by cathodoluminescent topography [21]. Probably, in homoepitaxial InGaN samples, this factor is not involved, and the tail formation is not typical. On the other hand, the efficiency of PL emission is found to be lower in homoepitaxial samples. This can be an indication that tail states are important to provide more efficient radiative recombination. Recently the comparison of the InGaN QW materials has been reported with different dislocation density but on the

Table 2. Parameters of band tail in GaN and InGaN epitaxial structures. ΔE is the temperature-induced *blue* spectral shift; $E_0(0)$ and σ are fitting parameters (see text).

Structure	Method	Indium content, %	ΔE, meV	$E_0(0)$, eV	σ, meV
GaN, thick ($\sim$ 1 μm) epilayer	PL	0	$\sim$0	$\sim$3.48	< 2
InGaN, DH, d=40 nm[a]	PL	2	$\sim$3	3.432	8
InGaN:Si, SH[b]	PL	6	6	3.387	13.7
InGaN, MQW, d is not indicated[c]	PL	$\sim$20	7.6	$\sim$3.4	6.5
InGaN, SH, d=110 nm (SH #5743)	PL	8.5±1.5	20	3.34	10
InGaN, DH, d=40 nm (DH #5748)	PL	7.5±1.5	30	3.289	14.5
InGaN, SH, d=200 nm[d]	PL	20	24	3.05	16
InGaN, SQW, d=2.5 nm (LED #302)[e]	EL	15–30	52	2.78	31.5
InGaN, SQW, d=2.5 nm (LED #228)	EL	30–45	30	2.394	28.6
InGaN, SQW, d=2.5 nm (LED #229)[e]	EL	30–45	59	2.392	35
InGaN, 10-MQW, d=3 nm (Homoepitaxy)	PL	$\sim$20	0	3.036	$\sim$0

[a] Derived from PL spectral peak position plot in Ref. [11]. [b] Derived from PL measurements reported in Ref. [14]. [c] PL study reported in [15]. Peak position of 3.4 eV suggests lower In content than value of 20% indicated in the paper. [d] Derived from experimental plots in Ref. [16]. [e] Derived from EL measurements (see [13]). The In content is known rather roughly.

same epitaxial wafer (prepared using so called *lateral epitaxial overgrowth* technique) [22]. It has not been found difference in optical properties of such materials and concluded that the effective band gap fluctuation in InGaN QWs is not related to threading dislocations. However, in that experiment the regions of high dislocation density are rather narrow stripes (5 μm wide) surrounded by "lateral-overgrown" low-dislocation material. Therefore, the comparable study is not easy because of scattering of both pumping and emitted light in the material. More reliable result could be obtained by comparison of characteristics of separate samples. We use this way comparing InGaN material grown on sapphire and on GaN bulk crystals. Certainly, there are also issues of different growth condition, layer thickness, and average indium content of separate samples.

6 Conclusions

Similarly to GaN, the InGaN alloy emits interband radiation in spite of very high density of defects, demonstrating low sensitivity of the radiation yield to the dislocation density. But this alloy emits even better than GaN, and it has advantage in laser diode applications. Large-scale production of short-wavelength LEDs is based on utilization of InGaN quantum wells. Commercial production of InGaN QW LDs is announced this year. In researches, the emission characteristics of InGaN are understood in terms of localized states adjacent to the nominal edge of the interband transitions in the quantum well. Our point is to treat these states as a band tail with smooth DOS distribution. A new finding is that in homoepitaxial InGaN QWs there is no anomalous "blue" temperature-induced spectral shift, which is typical for sapphire-substrate samples. This is an indication that inhomogeneous broadening can be associated with features of homoepitaxial growth (no misfit stress to the substrate, lower dislocation density). Dislocations seem to be involved in the formation of tail states, however further study is necessary for deeper understanding of their role.

Acknowledgments

Author is thankful to his colleagues by the nitride-related researches I. V. Akimova of P. N. Lebedev Physics Institute, Moscow, Russia, Dr. M. Osinski, Dr. E. Rabinovich and J. Lee of UNM, Albuquerque, NM, Prof. S. Sakai, Dr. S. Juodkazis and T. Sugahara of University of Tokushima, Japan, Dr. P. Perlin of Unipress, Warszawa, Poland. For useful discussions author thanks Dr. S. Nakamura of Nichia Res. Center, Anan, Japan, Prof. S. Fujita and Dr. Y. Kawakami of Kyoto University, Kyoto, Japan.

References

[1] S. Nakamura, M. Senoh, N. Iwasa and S. Nagahama, *Jpn. J. Appl. Phys.* **34**, L797-L799 (1995)

[2] S. Nakamura, M. Senoh, S. Nagahama, N. Iwasa, T. Yamada, T. Matsushita, H. Kiyoku, Y. Sugimoto, *Jpn. J. Appl. Phys.* **35** (1B) Pt. 2, L74-L76 (1996).

[3] I. Akasaki, S. Sota, H. Sakai, T. Tanaka, M. Koike and H. Amano, *Electron. Lett.* **32** (12) 1105-1106 (1996).

[4] S. Nakamura, M. Senoh, S. Nagahama, N. Iwasa, T. Matsushita and T. Mukai, *Proc. 2 nd Int. Symp. "Blue Lasers and Light Emitting Diodes"* Sep. 29 - Oct. 2, 1998, Chiba, Japan 371-376 (1998).

[5] S. Nakamura and G. Fasol, *The Blue Laser Diode* Springer-Verlag, Berlin, 1997.

[6] K. Osamura, K. Nakajima, Y. Murakami, P. H. Shingu, A. Ohtsuki, *Solid State Commun.* **22**, 617-621 (1972).

[7] K. Osamura, S. Naka and Y. Murakami, *J. Appl. Phys.* **46**, 3432 (1975).

[8] I. Ho and G. B. Stringfellow, *MRS Symp. Proc.* **449**, 871 (1997).

[9] I. V. Akimova, P. G. Eliseev and M. Osinski, *Quant. Electronics* (Moscow) **28** (11) 1013-1016 (1998).

[10] A. Bykhovski, B. Gelmont and M. Shur, *J. Appl. Phys.* **74**, 6734 (1993).

[11] Y. Narukawa, S. Saijou, Y. Kawakami, S. Fujita, T. Mukai and S. Nakamura, *Appl. Phys. Lett.* (1999).

[12] I. V. Akimova, P.G. Eliseev, M. A. Osinski, P. Perlin, *Quant. Electron.* **26** (12), 1039-1041 (1996).

[13] P. G. Eliseev, P. Perlin, J. Lee, M. Osinski, *Appl. Phys, Lett.* **71** (5), 5659-571 (1997).

[14] T. Taguchi, T. Maeda, Y. Yamada, S. Nakamura, G. Shinomiya, *Int. Symp. Blue Lasers and LEDs*, Chiba Univ., Japan, 1996, Proc., 372-374 (1996).

[15] K. L. Teo, J. S. Colton, P. Y. Yu, E. R. Weber, M. F. Li, W. Liu, K. Uchida, H. Tokunaga, N. Akutsu and K. Matsumoto, *Appl. Phys. Lett.* **73** (12), 1697-1699 (1998).

[16] S. Chichibu, L. Sugiura, J. Nishio, A. Setoguchi, H. Nakanishi and K. Itaya, *Proc. 2 nd Int. Symp. Blue Lasers and LEDs*, Chiba, Japan, 616-619 (1998).

[17] M. Osinski, P. G. Eliseev, P. Perlin, J. Lee, H. Sato, T. Sugahara, Y. Naoi, S. Sakai, *Adv. Program of CLEO/IQEL'1998*, San Francisco, CA, May 3-8, 1998, Pap. CWH5, pp. 107 (1998).

[18] T. Sugahara, P. G. Eliseev, H. Saeki, Y. Naoi, K. Nishino and S. Sakai, *46 th Japanese Appl. Phys. Conf.* Noda Campus, Tokyo Sci. University, March 28-31 (1999).

[19] P. G. Eliseev, I. V. Akimova, P. Perlin and M. Osinski, *3rd All-Russian Conf. Semicond. Physics*, Moscow, 1-5 Dec., 1997; Abstr., p. 88 (1997).

[20] H. Sato, T. Sugawara, Y. Naoi, S. Sakai, *Jpn. J. Appl. Phys.* **37** (4A), 2013-2015 (1998).

[21] T. Sugahara, M. Hao, T. Wang, D. Nakagawa, Y. Naoi, K. Nishino, S. Sakai, *Jpn. J. Appl. Phys.* **37** (10B), L1195-L1198 (1998).

[22] S. F. Chichibu, H. Marchand, M. S. Minsky, S. Keller, P. T. Fini, J. P. Ibbetson, S. B. Fleischer, J. S. Speck, J. E. Bowers, E. Hu, U. K. Mishra, S. P. DenBaars, T. Deguchi, T. Sota and S. Nakamura, *Appl. Phys. Lett.* **74** (10), 1460-1462 (1999).